

Impact of molecular structure, headgroup and alkyl chain geometry, on the adsorption of the anionic ester sulfonate surfactants at the air-solution interface, in the presence and absence of electrolyte.

Zi Wang^{1,2}, Peixun Li², Kun Ma², Yao Chen², Mario Campana², Jeffrey Penfold^{2,3,†}, Robert K Thomas³, David W Roberts⁴, Hui Xu⁵, Jordan T Petkov⁶, Zifeng Yan^{1,†}

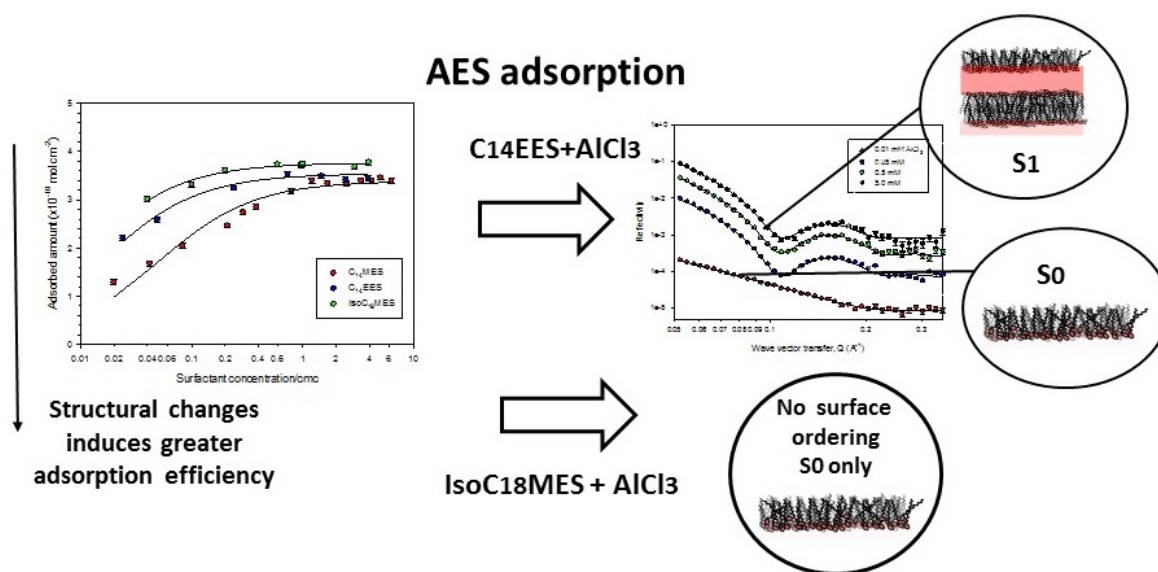
1. School of Science, State Key Laboratory of Heavy Oil Processing, China University of Petroleum , Qingdao 266580, China
2. ISIS Facility, Rutherford Appleton Laboratory, STFC, Didcot, OXON, UK, OX11 0QX
3. Physical and Theoretical Chemistry Laboratory, Oxford University, South Parks Road, Oxford, UK, OX1 3QZ
4. School of Pharmacy and Biomolecular Sciences, Liverpool John Moores University, Liverpool, L3 3AF, UK
5. KLK Oleo, SDN BDH, Menara KLK, Muliara Damansara, 47810 Petaling, Jaya Selanger, Malaysia
6. Lonza UK, GB-Blackley, Manchester, Lancs, M9 8ES, UK

! Joint Corresponding Authors: Jeff Penfold, email: jeff.penfold@stfc.ac.uk, Yan Zifeng, email: zfyancat@upc.edu.cn

Keywords: ester sulfonate anionic surfactants, adsorption, air-solution interface, neutron reflectivity, surface multilayers

GRAPHICAL ABSTRACT

Impact of molecular structure, headgroup and alkyl chain geometry, on the adsorption of the anionic ester sulfonate surfactants at the air-solution interface, in the presence and absence of electrolyte.



ABSTRACT.

The transition from monolayer to multilayer adsorption at the air-water interface in the presence of multivalent counterions has been demonstrated for a limited range of anionic surfactants which exhibit increased tolerance to precipitation in the presence of multivalent counterions. Understanding the role of molecular structure in determining the transition to surface ordering is an important aspect of the phenomenon. The focus of the paper is on the alkyl ester sulfonate, AES, surfactants; a promising group of anionic surfactants, with the potential for improved performance and biocompatibility. Neutron reflectivity measurements were made in aqueous solution and in the presence of NaCl, CaCl₂, MgCl₂ and AlCl₃, for a range of alkyl ester sulfonate surfactants, in which the headgroup and alkyl chain geometries were manipulated.

In the regions of monolayer adsorption changing the AES headgroup and alkyl chain geometries results in an increased saturation adsorption and in a more gradual decrease in the adsorption at low concentrations, consistent with a greater adsorption efficiency. Changing the AES headgroup and alkyl chain geometries also results in changes in the transition from monolayer adsorption to more ordered surface structures with the addition of AlCl₃ and mixed multivalent electrolytes. A more limited surface layering is observed for the ethyl ester sulfonate, EES, with a C₁₄ alkyl chain. Replacing the C₁₄ alkyl chain with a C₁₈ isostearic chain results in only monolayer adsorption.

The results demonstrate the role and importance of the surfactant molecular structure in determining the nature of the surface adsorption in the presence of different electrolytes, and in the tendency to form extended surface multilayer structures.

(1) INTRODUCTION

The major surface active ingredients in most home and personal care products are anionic surfactants (1, 2). Although formulations are usually mixtures of different anionic and non-ionic surfactants (3, 4), the structure, the surface activity and functionality of the anionic surfactant are important factors in determining overall performance (1, 2). Through changes in alkyl chain length and structure and headgroup structure, the structure of anionic surfactants has evolved to provide improved detergency, enhanced low temperature performance, improved biocompatibility and biodegradability, and improved tolerance to hard water conditions (1, 2). Of particular interest and relevance to this paper is the effect of multivalent ions on anionic surfactants. This is usually associated with hard water tolerance, but the focus is different here. The linear saturated alkyl chain surfactants, especially the longer alkyl chain lengths rapidly precipitate due to strong binding and complexation with the multivalent ions (5-9). The development of the alkyl benzene sulfonates, LAS, (1, 2, 10) and the alkyl ethoxy ether sulfates, SLES, (5, 11-13) has led to greater tolerance to precipitation in the presence of multivalent ions, and LAS has also demonstrated improved detergency and biodegradability (1, 2). More recently the methyl ester sulfonates, MES, surfactants have been promoted as replacements for anionic surfactants such as LAS (14, 15) in home and personal care products for which optimised detergency is an important criterion. Recent studies have demonstrated better cold water detergency, hard water tolerance and greater biodegradability (16-20), and the synthesis from sustainable sources (21). Hence the synthesis, purification, adsorption and self-assembly properties have been extensively studied (22-27).

An important feature of the anionic surfactants which show a greater tolerance to precipitation in the presence of multivalent counterions is the formation of surface multilayer structures with the addition of multivalent counterions (28-36), and is the focus of this paper. The surface multilayer formation is also associated with extreme and persistent wetting of hydrophobic surfaces (37), and has important consequences for efficient surface delivery and retention of different active components, such as perfumes (38). The surface multilayer formation occurs at low surfactant concentrations and largely outside the regime of precipitation, due to strong complexation with the multivalent counterions, as discussed in detail elsewhere (28). It has been demonstrated for different LAS isomers, and in LAS / non-ionic surfactant mixtures with the addition of Ca^{2+} counterions (29-31), and for SLES (32-35) and MES (36, 37) with the addition of Al^{3+} counterions. Within that range of studies the impact of some aspects of the surfactant structure have been explored.

For the SLES surfactants the impact of the headgroup geometry (33) and the alkyl chain length (34) on the surface layering induced in the presence of AlCl_3 was explored. For sodium diethylene glycol monododecyl ether sulfate, SLE_2S , with increasing AlCl_3 concentration the surface structure evolved from a monolayer, S_0 , to a monolayer with 1 to 3 bilayers beneath the initial monolayer, S_1 and S_3 , and ultimately to extended multilayer structures, S_n , where n is >20 (33). Similar transitions were observed for the less hydrophilic sodium ethylene glycol monododecyl ether, SLE_1S , and for the more hydrophilic sodium triethylene glycol monododecyl ether, SLE_3S . Notably for the more hydrophilic SLE_3S the regions over which multilayer formation, and especially the S_1 and S_3 structures, are extended to higher AlCl_3 concentrations. This was attributed to the increased steric hindrance of the larger ethylene oxide group disrupting the $\text{SLES} / \text{Al}^{3+}$ complex formation. For the sodium diethylene glycol monoalkyl ether sulfate, SAE_2S , surfactant the nature of the adsorption in the presence of Al^{3+} counterions has been investigated for alkyl chain lengths varying from C_{10} to C_{16} (34). As observed with the changing SLES headgroup structure, reducing the alkyl chain length from dodecyl, C_{12} , to decyl, C_{10} , results in a less hydrophobic surfactant and an extension of the formation of the multilayer structures to higher AlCl_3 concentrations. Correspondingly increasing the alkyl chain length from decyl to tetradecyl, C_{14} , results in surface multilayer formation occurring at lower surfactant and AlCl_3 concentrations. For the longer alkyl chain lengths, C_{14} and C_{16} , the decrease in solubility and the closer proximity of the precipitation boundary ultimately dominate the surface behaviour and the multilayer formation occurs over a narrower range of AlCl_3 concentrations.

The addition of electrolyte to the alkyl 2-sulfo-1-methyl ester, MES, surfactants results in adsorption trends (27, 36, 37) similar to those reported for the SLES surfactants (32-35). In the presence of NaCl and CaCl_2 only monolayer adsorption is observed, with an increased adsorbed amount. The addition of AlCl_3 to the C_{14}MES surfactant results in the formation of layered structures at the interface, in which the evolution in the structural form varies with AlCl_3 and surfactant concentration (36). With increasing AlCl_3 concentration the surface structure evolves from a monolayer, S_0 , to different multilayer structures with increasing long range order, comprising of a monolayer with 1 to 3 bilayers, S_1 to S_3 , beneath the initial monolayer and eventually to a multilayer structure, S_n , with a relatively large number of bilayers, >20 . Increasing the alkyl chain length from C_{14} to C_{16} and C_{18} results in a more limited range of multilayer structures, as the proximity of precipitation is closer for the longer alkyl chain lengths. For C_{16}MES and the eutectic mixture of C_{16}MES and C_{18}MES (37) only the

transition from monolayer adsorption to a surface structure comprising an initial monolayer and a single bilayer beneath the monolayer, S_1 , is observed.

These limited studies show that manipulating the surfactant geometry, through changes to the headgroup and alkyl chain structure, can have a significant impact upon the nature of the surface adsorption induced by the presence of multivalent counterions. The focus of this paper is to further investigate the impact of molecular structure on the surface adsorption and the structure of the adsorbed layer in the presence of multivalent counterions. In particular we have explored the role of an branched isostearic alkyl chain compared to a linear saturated alkyl chain, and on the modification of the headgroup geometry from methyl ester to ethyl ester in the MES surfactant.

(2) EXPERIMENTAL DETAILS

(i) Surface tension

Surface tension measurements were made for $C_{14}EES$ and $isoC_{18}MES$ in H_2O and in 0.1 M NaCl using a Kruss K100 maximum pull tensiometer with a platinum plate. The plate was rinsed in high purity water and dried in a Bunsen flame before each measurement. The tensiometer was calibrated for a surface tension of pure water of 72 mNm^{-1} . The temperature was controlled to $25 \pm 1^\circ\text{C}$ and repeated measurements were made at each concentration until the variation in the surface tension was $\leq 0.2 \text{ mNm}^{-1}$. The values plotted are the average values and the associated error is $\leq 0.1 \text{ mNm}^{-1}$.

(ii) Neutron Reflectivity

The neutron reflectivity, NR, measurements were made on the SURF reflectometer (39) at the ISIS pulsed neutron source. The reflectivity, $R(Q)$, was measured as a function of the wave vector transfer perpendicular to the surface, Q ; where Q is defined as $Q=4\pi\sin\theta/\lambda$, and θ is the grazing angle of incidence and λ the neutron wavelength. The measurements were made at a fixed θ of 1.5° and for wavelengths from 1 to 7 Å, sorted by time of flight, to cover a Q range ~ 0.05 to 0.35 Å^{-1} . The reflectivity was converted to an absolute scale by reference to the direct beam and the reflectivity from a D_2O surface. The measurements were made in null reflecting water, nrw, a 8 mole% D_2O / 92 mole% H_2O mixture with a scattering length density or refractive index matched to air. The measurements were made in sealed Teflon troughs with sample volumes $\sim 25 \text{ mL}$ and at a temperature of $25 \pm 0.5^\circ\text{C}$. The measurements were made

sequentially on a 7 position sample changer and repeated ~2-3 times until the reflectivity had reached a steady state. Each individual measurement took ~ 20 to 30 mins, and this resulted in a total lapse time in the measurements ~ 3- 6 hrs.

(iii) Materials

The two surfactants used, sodium tetradecanoic 2-sulfo 1-ethyl ester, C₁₄EES, and sodium isostearic 2-sulfo 1-methyl ester, isoC₁₈MES, were synthesised with the alkyl chains deuterium labelled, with chemical formula, C₁₄D₂₆H₅SO₅Na, and C₁₈D₃₄H₃SO₅Na, respectively; and the corresponding structures are shown in figure 1 (shown also is the previously studied Sodium tetradecanoic 2-sulfo 1-methyl ester, C₁₄MES, for comparison). The isoC₁₈MES is shown in figure 1 as a single isomer, but the material is a mixture of branched isomers, predominantly with the methyl branch distributed along the chain.

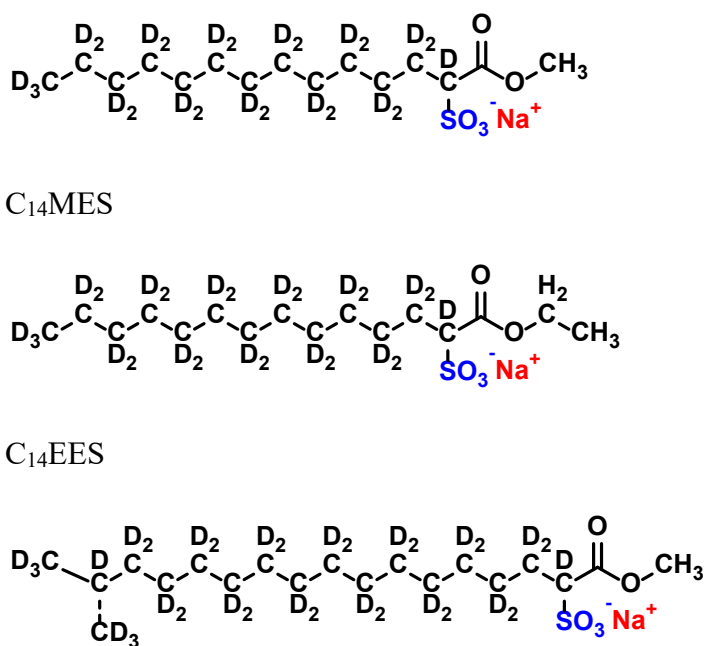


Figure 1. Structure of C₁₄MES, C₁₄EES and isoC₁₈MES

The synthesis and purification of the C₁₄EES and isoC₁₈MES follow that previously described for C₁₄MES (27). The surfactants were synthesised by direct sulfonation of the deuterated tetradecanoic ethyl ester and the deuterated isostearic methyl ester by SO₃ introduced from the vapour phase. The corresponding ethyl and methyl esters were produced using deuterated tetradecanoic acid and deuterated isostearic acid and non deuterated ethanol or methanol.

Deuterium oxide, D₂O, was obtained from Sigma Aldrich and high purity water (ElgaUltrapure with a resistivity of 18.2 MΩcm) was used. Analytical grade (>99.9% purity) NaCl, CaCl₂, MgCl₂ and AlCl₃ were obtained from Sigma-Aldrich and used as supplied. All glassware, Teflon troughs and other containers used in the NR measurements and sample preparation were cleaned in alkali detergent (Decon90) and extensively rinsed in ultrapure water.

(iv) Measurements made

NR measurements were made for deuterated C₁₄EES in nrw over the concentration range 0.05 to 8 mM, and for deuterated isoC₁₈-MES in nrw over the concentration range 0.02 to 2 mM, in order to determine the nature of their adsorption isotherms. Further measurements were made for C₁₄EES in nrw with 100 mM NaCl (for surfactant concentrations from 0.01 to 1 mM), with 5 mM CaCl₂ and 5 mM MgCl₂ (for surfactant concentrations from 0.001 to 0.6 mM); and for isoC₁₈MES with 100 mM NaCl (for surfactant concentrations from 0.001 to 0.6 mM) and in 0.005 and 0.1 mM CaCl₂ (for surfactant concentrations from 0.001 to 0.6 mM).

A series of NR measurements were made for C₁₄EES and isoC₁₈MES in nrw in the presence of AlCl₃; at surfactant concentrations of 0.1, 0.5, and 1.0 mM and AlCl₃ concentrations from 0.005 to 5 mM for C₁₄EES, and for 0.1, 0.2, 0.3, 0.5 and 1.0 mM isoC₁₈MES and AlCl₃ concentrations from 0.001 to 20 mM.

Additional NR measurements were made for C₁₄EES in nrw in the presence of electrolyte mixtures, AlCl₃ / CaCl₂ and AlCl₃ / MgCl₂; at a surfactant concentration of 0.5 mM and 1 mM; in the presence of either 5mM CaCl₂ or MgCl₂ and for AlCl₃ concentrations from 0.05 to 5 mM.

Surface tension measurements were made for C₁₄EES and isoC₁₈MES in H₂O and in 0.1 M NaCl.

(3) RESULTS and DISCUSSION

(i) Surface tension

The surface tension data for C₁₄EES and isoC₁₈MES in H₂O and in 0.1 M NaCl are shown in figure S1 in the Supporting Information. The onset of the formation of micelle aggregates is indicated by the sharp break in the surface tension data, as characterised by the critical micellar concentration, cmc. The derived cmc values are summarised in table S1a in the Supporting

Information. For both the C₁₄EES and isoC₁₈MES the expected shift in the cmc and the surface tension at the cmc to lower values in the presence of 0.1 M NaCl are observed.

Previously Roberts (40) has shown that the micellisation potential, as expressed as the negative logarithm of the cmc, $\text{p}cmc$, is a function of the hydrophobicity of the surfactant components, and that the hydrophobicity can be modelled by the logP value, octanol-water partition coefficient, of the different hydrophobic portions of the surfactant. This has been applied here, and details of the calculation followed can be found in reference 40. There is good agreement with the measured cmc values for C₁₄-MES, C₁₄-EES, and isoC₁₈-MES, as summarised in table S1b in the Supporting Information.

(ii) Monolayer adsorption

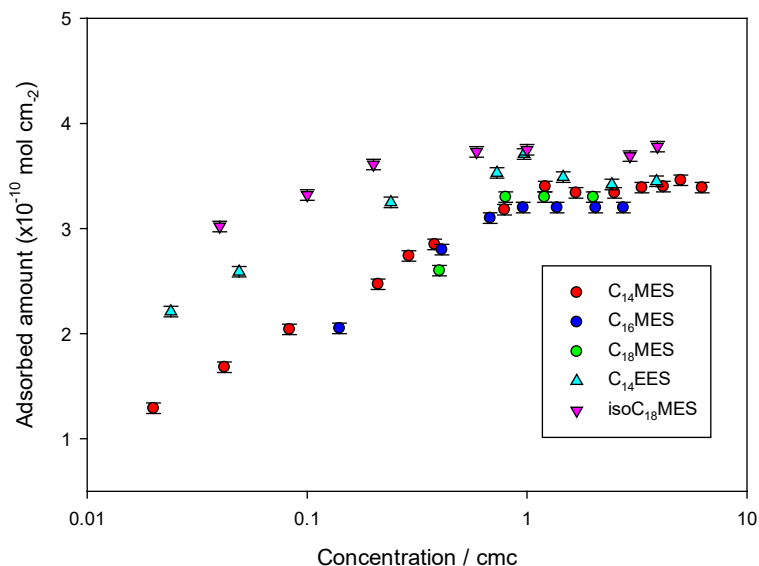
The adsorption isotherms, at concentrations from below to in excess of the cmc, were measured for C₁₄EES and isoC₁₈MES by NR. The measurements were made in nrw using alkyl chain deuterium labelled surfactants. As demonstrated extensively elsewhere (41) the resulting reflectivity arises only from an adsorbed layer at the interface. The data are consistent with a thin monolayer, ~ 20 Å, and are modelled, using the exact optical equations for a thin film at the interface (41), as a thin layer of uniform composition to give a thickness, d , and a scattering length density, ρ . A flat background is also included in the modelling. Hence there are three refinable parameters, d , ρ and the background. It is well established that the adsorbed amount, Γ , or area/molecule, A , is determined to good accuracy from the $d \cdot \rho$ product (41), such that $A = \sum b / d \cdot \rho$ and $\Gamma = 1 / N_A A$ (where N_A is Avogadro's number and $\sum b$ is the sum of scattering lengths of the adsorbed component, see table 1 for the values used in this study).

Table 1. $\sum b$ values for surfactants used in this study

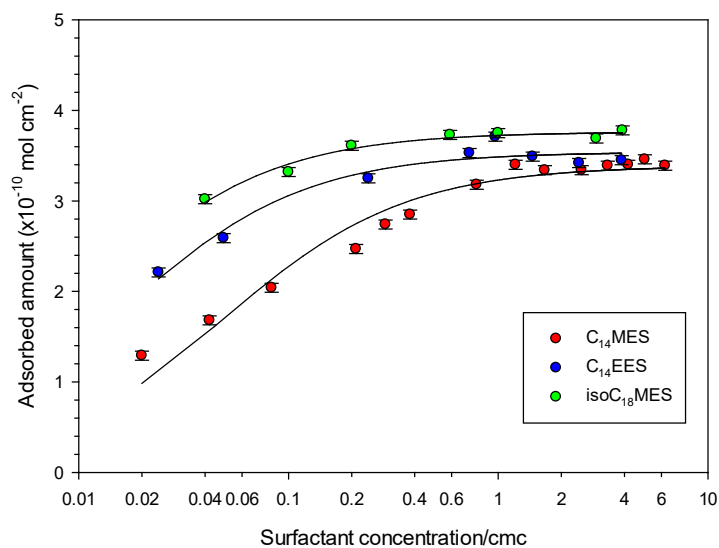
Surfactant	$\sum b$ ($\times 10^{-3}$ Å)
C ₁₄ EES	2.966
isoC ₁₈ MES	3.77

The key model parameters are summarised in table 2 in the Supporting Information, and the associated adsorption isotherms are presented in figure 2a along with those from previous

measurements for $C_{14}MES$, $C_{16}MES$ and $C_{18}MES$ (27, 37). The concentration axes are scaled to their respective cmc values (2.06 mM for $C_{14}EES$, 0.59 mM for $isoC_{18}MES$, 2.40, 0.78 and 0.25 mM for C_{14} , $C_{16}MES$ and $C_{18}MES$ respectively).



(a)



(b)

Figure 2. (a) Adsorbed amount, Γ , ($\times 10^{-10} \text{ mol cm}^{-2}$) versus surfactant concentration scaled to cmc for $C_{14}MES$, $C_{14}EES$, $C_{16}MES$, $C_{18}MES$ and $isoC_{18}MES$ (see legend for details). The data for $C_{14}MES$, $C_{16}MES$ and $C_{18}MES$ are reproduced from references 27, 36 and 37. (b) Adsorbed amount, Γ , ($\times 10^{-10} \text{ mol cm}^{-2}$) versus surfactant concentration scaled to cmc for

C₁₄MES, C₁₄EES, and isoC₁₈MES (see legend for details). The solid lines are fits to a Langmuir isotherm, using the parameters in table 2. Although included in the figure, for clarity the mean error in the adsorbed amount is $\pm 0.05 \times 10^{-10} \text{ mol cm}^{-2}$.

The mean thickness of the adsorbed layer is, $\sim 19 \pm 1 \text{ \AA}$ for C₁₄EES and $\sim 21 \pm 1 \text{ \AA}$ for isoC₁₈MES. The adsorbed layer thickness for C₁₄EES is similar to that reported for C₁₄MES, $20 \pm 1 \text{ \AA}$ (27, 36). The thickness of the isoC₁₈MES layer is slightly larger, reflecting the longer alkyl chain length. However, in all cases and also for the previously reported C₁₆MES and C₁₈MES (37) the variations are within the experimental errors. Furthermore the variations in the adsorbed layer thickness with surfactant structure are partially masked by the surface roughness contribution (41).

In figure 2b the adsorption data for C₁₄MES, C₁₄EES and isoC₁₈MES are plotted and modelled using a Langmuir isotherm in the form $\Gamma = \Gamma_{\text{max}} C / (k_d + C)$, where Γ , Γ_{max} are the adsorbed amounts and saturation adsorption, C is the surfactant concentration and k_d the adsorption coefficient (42). The concentration axis in figure 2b is scaled to the cmc values of the individual surfactants. The key parameters from the fits to a Langmuir isotherm are summarised in table 2. The Gibbs free energy of adsorption, ΔG_{ads} , calculated from $\Delta G_{\text{ads}} = -RT \ln(k_d)$, is also included in table 2.

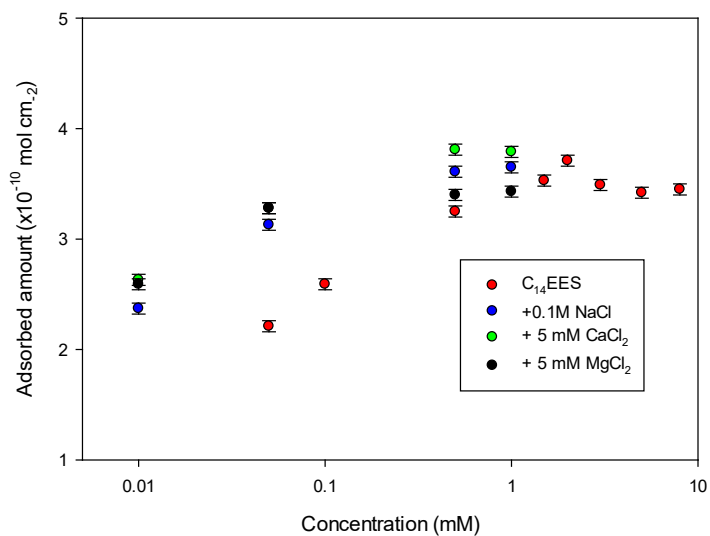
Table 2. Langmuir adsorption isotherm parameters for data in figure 2b.

Surfactant	Γ_{max} ($\pm 0.05 \times 10^{-10}$ mol cm ⁻²) ^a	Γ_{max} ($\pm 0.05 \times 10^{-10}$ mol cm ⁻²) ^b	Cmc (± 0.02 mM)	k_d	ΔG_{ads} (kJ)
C ₁₄ EES	3.48	3.54	2.06	0.016	-4.14
isoC ₁₈ MES	3.71	3.76	0.51	0.010	-4.61
C ₁₄ MES	3.40	3.39	2.40	0.049	-3.02

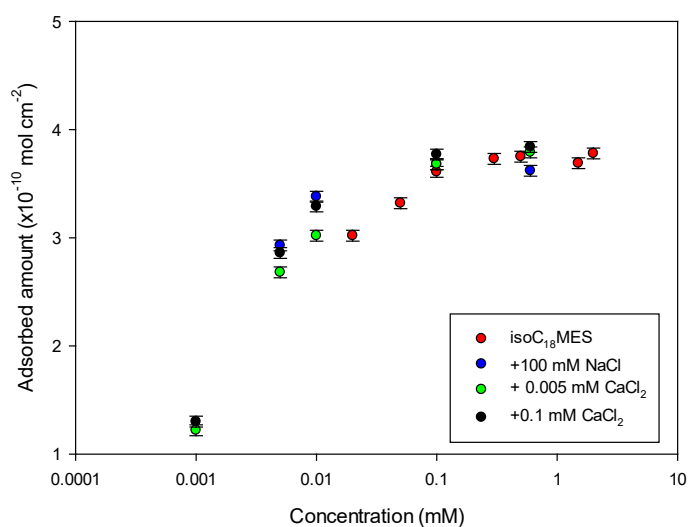
a. Average of data points above the cmc. B. From fit to Langmuir isotherm

There is a good correspondence between the maximum or saturation adsorption derived from the fit to the Langmuir isotherm and the average of the data points above the cmc. It was previously shown that the saturation adsorption for the MES surfactants with alkyl chain lengths of 14, 16, and 18 were within error in close agreement; with values of 3.4 , 3.2 and $3.3 \pm 0.1 \times 10^{-10} \text{ mol cm}^{-2}$ respectively (37). Here the saturation adsorption for C₁₄EES, 3.48×10^{-10}

mol cm⁻², is similar to that for C₁₄MES, but that of isoC₁₈MES, 3.71 x10⁻¹⁰ mol cm⁻², is significantly higher. It was previously observed (37) that the invariance in the adsorption isotherms and saturation adsorption for the C₁₄, C₁₆, and C₁₈MES surfactants implies that the saturation adsorption is determined by the alkyl chain packing and that the headgroup plays a more secondary role. This is further reinforced by the results for C₁₄EES which are similar to the MES data. This implies that changing from a methyl to an ethyl group in the headgroup structure has relatively little impact upon the monolayer packing at saturation. The notable difference observed is the increase in the saturation adsorption for the isoC₁₈MES. In this case the branching of the alkyl chain results in a more compact packing at the interface. However, the significant feature in the data in figure 2b and the corresponding Langmuir isotherm fits is the different slopes in the adsorption below the cmc. That is, the decrease in the adsorption with decreasing concentration is increasingly less pronounced going from C₁₄MES to C₁₄EES to isoC₁₈MES. This reflected in the value of the adsorption coefficient, k_d , which decreases from 0.049 to 0.010 going from C₁₄MES to isoC₁₈MES (see table 2). That is, as k_d becomes smaller a lower bulk surfactant concentration is required to obtain the same degree of surface coverage, and so the surface affinity or surfactant efficiency increases. This is also reflected in the variation in the ΔG_{ads} values, which are systematically higher for C₁₄EES and isoC₁₈MES compared to C₁₄MES, and quantifies the greater tendency towards adsorption as the headgroup and alkyl chain geometries are altered. This is different to what is observed in the alkyl methyl sulfonate series, with alkyl chains from C₁₄ to C₁₈ (37) in the alkyl sulfates, SAS, (43) and the alkyl ethoxy sulfates, SLES, surfactants (34, 45), where the isotherms for the different alkyl chain lengths all overlap. The physical origins of these significant differences in the form of the isotherm are uncertain, but are often discussed in the context of other description of the adsorption isotherm such as Van der Waals, or Frumkin (44) which include additional parameters to account for factors such as a strong interaction between alkyl chains or a net repulsion between neighbouring headgroups. It could also be interpreted as the difference between uniform and a patchy distribution of the molecules at the surface at partial coverage. Fainerman and Miller (46) have shown how the formation of n'mers at the surface results in a decrease in surface pressure with increasing n' mer formation, resulting in a more efficient surface adsorption. Although uniform coverage is assumed in the interpretation of the NR data, the impact of inhomogeneous lateral distributions has been extensively discussed (41), and the range of patch sizes encountered at partial coverage ensures that in terms of the interpretation of the NR data the assumption of a uniform distribution remains valid. We return to this point later when discussing the impact of electrolyte on the adsorption.



(a)



(b)

Figure 3. Adsorbed amount versus concentration (scaled to cmc) for (a) C₁₄EES and (b) isoC₁₈MES in NaCl, CaCl₂ and MgCl₂. (see legend for details). Although included in the figure, for clarity the mean error in the adsorbed amount is $\pm 0.05 \times 10^{-10} \text{ mol cm}^{-2}$.

In figures 3 a and b the impact of electrolyte, NaCl, CaCl₂ and MgCl₂, where monolayer adsorption still occurs, is shown for C₁₄EES and isoC₁₈MES. The key model parameters are summarised in table S2 in the Supporting Information.

The saturation adsorption for isoC₁₈MES in NaCl and CaCl₂ has hardly changed; 3.7×10^{-10} in the absence of electrolyte and 3.65×10^{-10} and 3.77×10^{-10} respectively in NaCl and CaCl₂. Furthermore for isoC₁₈MES the form of the isotherm in the presence of NaCl and CaCl₂ appears close to that observed in the absence of electrolyte. The results for isoC₁₈MES imply that the alkyl chain packing does dominate the adsorption and saturation adsorption value, and that decreasing the inter-headgroup repulsion by adding electrolyte has little impact. This is in contrast to what is usually observed in ionic surfactants (41, 45). The invariance in the adsorption of the isoC₁₈MES with added electrolyte suggests that the surfactant is behaving more like a non-ionic surfactant. It has already been shown that the lack of slope of the adsorption isotherm above the cmc for ionic surfactants (45) implies a more weakly ionic nature, as observed here for C₁₄EES and isoC₁₈MES, and this tendency was already reported for the MES surfactants (27, 37) and for the SLES surfactants (33, 34, 46). However the cmc in the presence of 0.1M NaCl has shifted from 0.59 mM to 0.01 mM (see table S1 and figure S1 in the Supporting Information). Furthermore when scaled to the respective cmc values the adsorption data with and without NaCl are quite different (see figure S2 in the Supporting Information).

In the presence of NaCl and CaCl₂ the saturation adsorption for C₁₄EES has increased from 3.48×10^{-10} mol cm⁻² in the absence of electrolyte to 3.63×10^{-10} and 3.79×10^{-10} respectively. In MgCl₂ there is little change in the saturation adsorption for C₁₄EES. Not only does the addition of NaCl and CaCl₂ increase the saturation adsorption for C₁₄EES, and by an amount similar to that observed for C₁₄MES, but the slope of the adsorption isotherm below the cmc has decreased. This is, in the presence of electrolyte, see figure 3a, due mainly to the expected decrease in the cmc with added electrolyte and the associated shift in the isotherm to lower concentrations (the isotherm data presented in figure 3 are not scaled to their respective cmc values). This is shown in the data points between 1 and 0.5 mM in figure 3a. The cmc for C₁₄EES in 0.1 M NaCl has decreased to 0.16 mM from 2.06 mM in the absence of electrolyte. The data presented in figure S2 in the Supporting Information shows the respective isotherms scaled to their associated cmc values, and the two isotherms coincide more closely than is the case for isoC₁₈MES.

For isoC₁₈MES the significant change in the cmc with added NaCl, and the significant change in the isotherms with and without NaCl when scaled to their respective cmc values appear inconsistent the minimal impact on the saturation adsorption of added electrolyte, and with the concept that the surfactant that it is acting like a non-ionic surfactant. The differences in the

isotherms scaled to their cmcs for isoC₁₈MES are not observed for C₁₄EES (see figure S2 in the Supporting Information). Furthermore for C₁₄EES the addition of electrolyte does have an impact upon the saturation adsorption, resulting in an increased adsorption. As discussed earlier this could be another manifestation of the concept of a patchy surface. However there is an additional factor to be considered. That is, the degree of counterion binding can be markedly different in the surface to its value in the associated micellar phase. In general the degree of counterion binding in the micelle is relatively low at the cmc and increases as the surfactant and micelle concentration increases, to give a mean value for the degree of ionisation of the micelle ~ 0.2 to 0.3 (45). However the surface can be constrained differently.

(iii) Surface ordering with AlCl₃

In the presence of AlCl₃ it has been previously demonstrated that surface ordering, the formation of surface multilayer structures, occurred for the SLES and MES surfactants (32-37, 47). Here the surface adsorption has been measured by NR in the presence of AlCl₃ for C₁₄EES and isoC₁₈MES at different surfactant concentrations and a range of AlCl₃ concentrations, where from the previous studies on MES (36, 37, 47) surface ordering might be expected. For C₁₄EES measurements were made at surfactant concentrations of 0.1, 0.5, 1.0 and 2.0 mM and for AlCl₃ concentrations in the range 0.005 to 5 mM.

At 0.1 mM C₁₄EES the surface adsorption in the AlCl₃ concentration range of 0.1 to 0.8 mM is in the form of a monolayer, and at 1.0 mM AlCl₃ a weak interference fringe is visible in the data, as summarised in table S3 and in figure S3 in the Supporting Information. The monolayer adsorption is described as a single layer of uniform composition, as described in the previous section, and in which the adsorbed amount is relatively constant. At 1.0 mM AlCl₃ the adsorption is described as a two layer structure; consistent with a monolayer ~ 20 Å thick and a thicker layer beneath it which corresponds to a partial weakly defined bilayer structure.

At the higher surfactant concentrations, 0.5, 1.0 and 2.0 mM, the reflectivity data are consistent with monolayer adsorption at the lowest AlCl₃ concentrations, and at the higher AlCl₃ concentrations the reflectivity data are dominated by a single pronounced interference fringe. The data for 0.5 and 1 mM surfactant concentration and a range of AlCl₃ concentrations are shown in figure 4 and figure S4 in the Supporting Information. The key model parameters from the analysis of the data at the surfactant concentrations from 0.5 to 2 mM are summarised in table S3 in the Supporting Information.

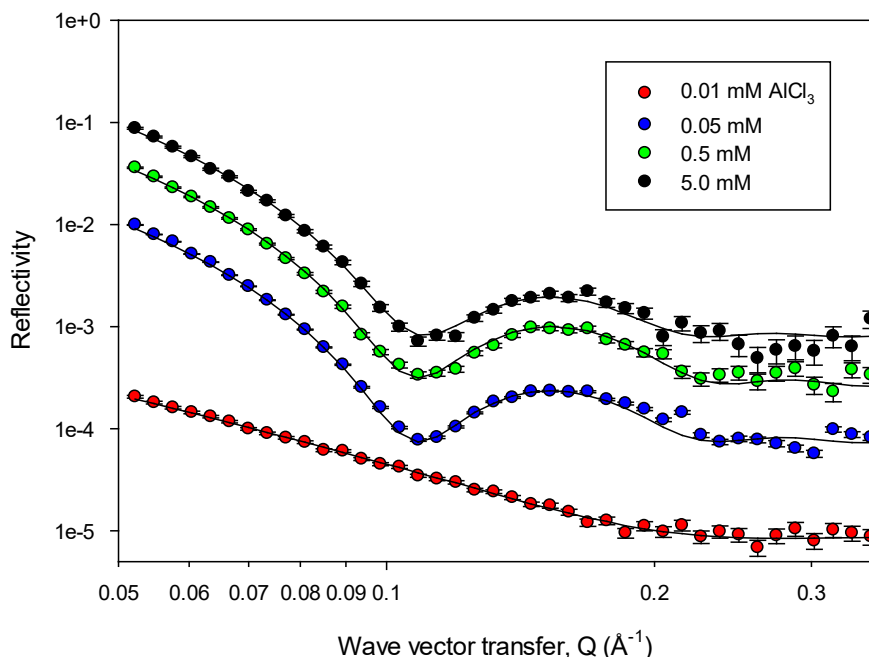


Figure 4. Neutron reflectivity for 0.5 mM $C_{14}EES$ in n_{rw} and $AlCl_3$ (see legend for details). The solid lines are model fits using the parameters summarised in table S3 in the Supporting Information, and the models described in the text. Each curve is shifted vertically by $\times 10$, $\times 40$, and $\times 100$ respectively for clarity.

The reflectivity data with the single pronounced interference fringe, with a minimum at a Q value $\sim 0.1 \text{ \AA}^{-1}$ is best described by 3 layers; comprising an initial monolayer at the interface with a bilayer adsorbed beneath it and separated from the initial monolayer by a thin mainly solvent layer. This is the S_1 structure designated in the Introduction, and extensively observed in the presence of $AlCl_3$ for the MES surfactants (36, 37, 47) and the SLES surfactants (32-35). What is notably different here is that as the $AlCl_3$ concentration is increased at a fixed surfactant concentration the transition from monolayer adsorption to the S_1 structure occurs at relatively low $AlCl_3$ concentration and no further structural transitions occur as the $AlCl_3$ concentration is increased up to 5 mM. Furthermore the S_1 structure that forms, within the errors in the range of model parameters that fit the data, shows no systematic variation with changing $AlCl_3$ concentration. This is in marked contrast to what has been previously observed for $C_{14}MES$ (36, 46) and for SLES (32-35), where an increase in the $AlCl_3$ concentration causes more extended surface structures to evolve from S_0 to S_1 - S_3 and ultimately to an extended multilayer structure, S_n . The transition from S_0 to S_1 and the absence of further structural

transitions can in part be rationalised by a tighter binding of the Na^+ counterion to the EES headgroup compared to the MES headgroup, or a hindering of the Al^{3+} ion binding by the bulkier headgroup. This is analogous to what was recently observed in the presence of mixed electrolytes ($\text{CaCl}_2 / \text{AlCl}_3$ and $\text{MgCl}_2 / \text{AlCl}_3$) where for C_{14}MES the structural transitions in the presence of CaCl_2 and MgCl_2 are shifted to higher AlCl_3 concentrations due to competitive counterion binding (46). It is well established that the monovalent and divalent counterions do not promote surface ordering in surfactants such as MES and SLES (32-37). It was also demonstrated (35) that different trivalent ions have different impacts on the surface ordering induced in SLES, dependent upon their relative binding strengths and hydrated radii. A more limited range of structures was observed for the $\text{C}_{16}\text{-C}_{18}\text{MES}$ eutectic mixture (37) and for the longer alkyl chain length SLES molecules in the presence of AlCl_3 (34). In those case it was attributed to the closer proximity of the precipitation boundary,

Similar measurements were also made for the $\text{isoC}_{18}\text{MES}$ surfactant at surfactant concentrations of 0.1, 0.2, 0.3, 0.5 and 1.0 mM and at AlCl_3 concentrations up to 20 mM, and the key model parameters are summarised in table S4 in the Supporting Information. In this case only monolayer adsorption was observed throughout the entire AlCl_3 and surfactant concentration range explored. Furthermore, as observed earlier for the addition of NaCl or CaCl_2 , the addition of AlCl_3 does not result in an enhanced monolayer adsorption. This implies that the Na^+ counterion is relatively tightly bound and is not easily displaced by the multivalent ions. This is similar to the observation that the divalent Ca^{2+} does not induce multilayer formation in the MES and SLES surfactants (32-37). Furthermore the observations are consistent with the more non-ionic or weakly ionic nature of the surfactant.

(iv) Surface ordering with $\text{AlCl}_3 / \text{CaCl}_2$, $\text{AlCl}_3 / \text{MgCl}_2$ mixtures

It was previously shown (47) that in the presence of mixed electrolytes, $\text{AlCl}_3 / \text{CaCl}_2$ mixtures for example, the pattern of surface ordering observed with increasing AlCl_3 concentrations was shifted to higher AlCl_3 concentrations. In light of the more limited range of surface structures observed for C_{14}EES , it is important to probe the impact of mixed electrolytes on the structural evolution for C_{14}EES . NR measurements were made at surfactant concentrations of 0.5 and 1.0 mM in 5mM CaCl_2 and 5 mM MgCl_2 for a range of AlCl_3 concentrations from 0.05 to 1.0 mM.

NR data showing the range of structures encountered in the $\text{CaCl}_2 / \text{AlCl}_3$ mixtures are shown in figure 5 at a surfactant concentration of 1 mM. Similar data are observed at the lower

surfactant concentration of 0.5 mM. The key model parameters from the analysis of these data are summarised in tables S5 a and b in the Supporting Information. As illustrated in figure 5, and in tables S5 a and b, the presence of CaCl_2 results in a more complex evolution in the surface structure as the AlCl_3 concentration is increased.

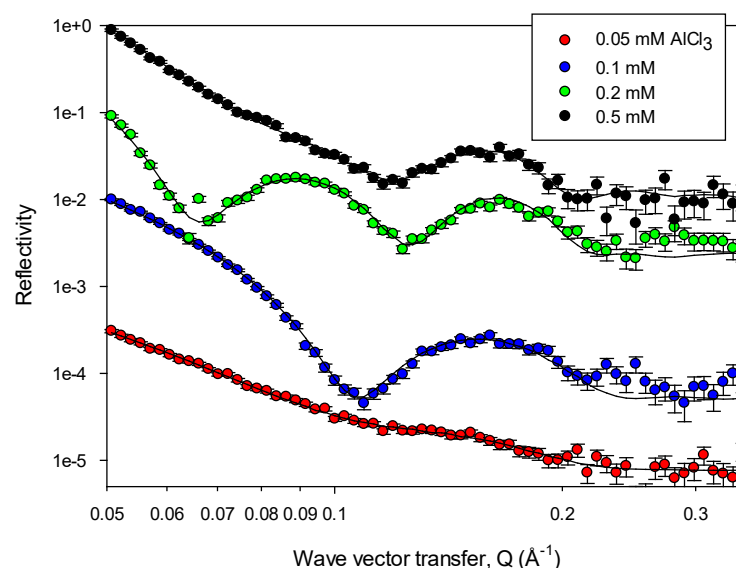


Figure 5. NR data for 1.0 mM C_{14}EES / 5 mM CaCl_2 and AlCl_3 concentrations from 0.05 to 0.5 mM (see legend for details). The solid lines are model fits, using the models described in the text, and the key model parameters summarised in table S5b in the Supporting Information.

Previously it was observed (47) that the addition of CaCl_2 or MgCl_2 shifted the pattern of the surface structural evolution to higher AlCl_3 concentrations for C_{14}MES . Here the addition of CaCl_2 at C_{14}EES surfactant concentrations of 0.5 and 1.0 mM results in the transition from monolayer, S_0 , to monolayer + bilayer, S_1 , structures at similar AlCl_3 concentrations to those encountered in the absence of CaCl_2 . However, instead of remaining at the S_1 structure, as shown in figure 4, with increasing AlCl_3 concentration there is now a transition to a more extended but discrete structure, S_2 , at intermediate AlCl_3 concentrations. This is characterised by a pronounced double interference fringe in the NR data, as illustrated in figure 5, with minima at Q values ~ 0.06 and 0.12 \AA^{-1} . The S_2 structure corresponds to an initial monolayer + 2 bilayers beneath, and is modelled as 5 discrete layers, see tables S5 a and b in the Supporting Information. At even higher AlCl_3 concentrations there is a transition back to the S_1 structure, which then remains invariant up to relatively high AlCl_3 concentrations.

A transition from more extended to less extended surface structures with increasing electrolyte has been previously reported for the SAES surfactants in AlCl_3 (34), but in rather different circumstances. It was observed for the more hydrophobic SAES surfactants with longer alkyl chain lengths, C_{14} , C_{16} , which were closer to precipitation. In that case at the high AlCl_3 concentrations a transition from extended multilayer structures, S_n , to monolayer adsorption, was observed, and was as a direct consequence of precipitation. The observations reported here for C_{14}EES in AlCl_3 / CaCl_2 mixtures are different and are associated with the competitive counterion adsorption which is modified by the presence of the ethyl rather than methyl ester group in the headgroup structure.

Interestingly, the NR data in the presence of AlCl_3 / MgCl_2 mixtures does not show the more complex structural evolution shown in figure 5 for AlCl_3 / CaCl_2 mixtures. For the AlCl_3 / MgCl_2 mixtures at surfactant concentrations of 0.5 and 1 mM, and in the presence of 5 mM MgCl_2 , the same single transition from monolayer, S_0 , to S_1 surface structures seen in the absence of MgCl_2 , is observed. The key model parameters are summarised in tables S6 and b in the Supporting Information. In AlCl_3 / MgCl_2 mixtures the transition from S_0 to S_n surface structures occurs at AlCl_3 concentrations of order 0.1 to 0.2 mM and 0.2 to 0.5 mM for surfactant concentrations of 0.5 and 1.0 mM respectively. However in the presence of AlCl_3 only the same transition occurs at lower AlCl_3 concentrations, ~ 0.01 to 0.5 mM and 0.005 to 0.05 mM for surfactant concentrations of 0.5 and 1 mM respectively.

(v) Discussion

It has been extensively reported (28, 32-37, 47) that the addition of Al^{3+} counterions to dilute C_{14}MES and SLES solutions promotes the formation of surface multilayer structures; from an initial monolayer, S_0 , to structures with a single bilayer beneath the monolayer, S_1 , up to extended multilayer structures, S_n , and often via intermediate structures with a small finite number of bilayers, S_2 , S_3 etc. The addition of the multivalent counterions promotes the formation of a concentrated surface multilayer structure at relatively low surfactant and counterion concentrations outside the regime of precipitation. The attractive force required to promote the concentrated surface multilayer structure from dilute solution arises from the strong binding of the multivalent counterions within the plane and through bridging across adjacent layers, resulting in a reduction in the surface free energy.

Here it is demonstrated that the $\text{isoC}_{18}\text{MES}$ shows no surface multilayer formation with the addition of Al^{3+} ions. For LAS the divalent Ca^{2+} was sufficient to promote surface multilayer

formation (29-31). Whereas for the SLES and MES surfactants it was not, and the stronger binding of the trivalent Al^{3+} was required. This implies that for isoC₁₈MES the Al^{3+} ions cannot substantially displace the Na^+ counterions in order to promote the required surface attractive interaction. Furthermore it is possible that the branched form of the alkyl chain hinders the formation of surface lamellar structures. It is known that changing the alkyl chain geometry does affect the ability to induce surface ordering, even though in the region of monolayer adsorption it results in a more dense layer, which might be thought of as an indicator for surface ordering. This was highlighted particularly with the dichain structure of the LAS surfactants (29-31) where the addition Ca^{2+} counterions induced surface layers. However it is difficult to separate the effect of counterion binding strength and alkyl chain geometry. For the eutectic C₁₆-C₁₈MES mixture (37) and for the SLES molecule with longer alkyl chain lengths (34) a more limited range of surface structures was also reported. In those cases this was associated with the closer proximity of the precipitation boundary. This is not the case here as the precipitation boundary is not close.

For the C₁₄EES surfactant only the S₀ and S₁ surface structures are observed with the addition of Al^{3+} , and so only a limited range of surface ordering occurs in the form of a single bilayer beneath the initial surface monolayer. This again can be attributed to a stronger binding of the Na^+ counterions compared to Al^{3+} . This could be associated with the change in the headgroup structure with the replacement of the methyl group with an ethyl group. Furthermore the bulkier headgroup could partially inhibit the binding of the multivalent counterions in and out of the plane. The impact of the relative binding strengths of different counterions in promoting or inhibiting surface multilayer formation has already been reported for Ca^{2+} / Al^{3+} mixtures (47) and for the different trivalent counterions (35). Similar changes were also reported for the SLES surfactants (33) through changes in the size of the polyethylene group associated with the headgroup. For the SLES surfactants the change in the local environment also resulted in a higher degree of counterion binding in the associated micellar phase.

The observations of the changes in surface structure in the presence of mixed ions, AlCl_3 / CaCl_2 and AlCl_3 / MgCl_2 , reinforces the importance of the relative binding strengths of the different counterions, and how this impacts upon the evolution in the surface structure. In the presence of AlCl_3 / MgCl_2 mixtures the shift to higher electrolyte concentrations for the transition from S₀ to higher order surface structures (see table S6 in the Supporting Information) is consistent with the previous observations for MES in AlCl_3 / CaCl_2 and AlCl_3 / MgCl_2 mixtures (47) and for SLES with different trivalent counterions (35). It is explained in

terms of the relative binding strengths and affinities of the different counterions present, Na^+ , Al^{3+} , and Mg^{2+} . Furthermore, as encountered with just Al^{3+} , only the S_1 structure is induced and more extended structures do not occur. In the presence of AlCl_3 / CaCl_2 mixtures the evolution in the surface structure is more complex, see figure 5. That is, with increasing electrolyte concentration the surface evolves from S_0 to S_1 to S_2 and back to S_1 . This is contrary to what is observed for C_{14}EES in AlCl_3 / MgCl_2 mixtures and for C_{14}MES in AlCl_3 / CaCl_2 and AlCl_3 / MgCl_2 mixtures (47). This is explained by the presence of the ethyl group as opposed to the methyl group in MES, providing an environment which subtly changes the balance between the relative binding strengths of Na^+ , Al^{3+} , and Ca^{2+} , but that the change is not sufficient to change substantially the balance between Na^+ , Al^{3+} , and Mg^{2+} . It is, for example, known from other studies (12) that Mg^{2+} binds less strongly to SLES than Ca^{2+} , and so is less effective in promoting micellar growth. The measurements in the mixed electrolytes are not made at a constant ionic strength. However the previous studies on SLES (32-34), on different counterions with SLES (35) and mixed counterions with MES (47) indicate that it is the nature of the counterions and their relative binding strength that are important and maintaining a constant ionic strength is less important.

From the form of the adsorption isotherms there is an implication that the $\text{isoC}_{18}\text{MES}$ and C_{14}EES surfactants reach saturation adsorption before the cmc is reached, which is a common feature of non-ionic surfactants (48), whereas SLES and C_{14}MES do not. Although previously assumed to be only mildly ionic (27, 36) SLES and C_{14}MES behave more like ionic surfactants and C_{14}EES and $\text{isoC}_{18}\text{MES}$ more like non-ionic surfactants.

The non-ionic character of the C_{14}EES and $\text{isoC}_{18}\text{MES}$ isotherms, as described earlier, and the relative invariance in the saturated adsorption with the addition of electrolyte seems at variance with the changes in the cmc with the addition of electrolyte. This can, however, be reconciled if the degree and strength of counterion binding at the surface and in micelles is different. That is, the degree of counterion binding at the surface is relatively high, whereas in the micellar phase it is relatively low.

The other important feature of the C_{14}EES and $\text{isoC}_{18}\text{MES}$ isotherms is the variation in the form of the adsorption isotherms at concentration values below the cmc, for the different surfactant geometries and with the addition of electrolyte. There is normally a coincidence in isotherms when scaled to their respective cmc's for homologous series; as observed for the alkyl sulfates, SLES and MES surfactants with different alkyl chain lengths (34, 37, 43). This

is illustrated in figure 2a for the C₁₄, C₁₆ and C₁₈ MES surfactants. The C₁₄EES and isoC₁₈MES surfactants do not follow that pattern, as shown in figure 2. This implies that changing the headgroup and alkyl chain structure respectively impact upon their adsorption efficiency. As such the adsorption efficiency, as measured by their respective adsorption coefficients, k_d , increase for C₁₄EES and isoC₁₈MES. That is, a lower surfactant concentration is progressively required to achieve the same degree of coverage. The invariance in the adsorption isotherm, when scaled to the respective cmc values, is also encountered with the addition of electrolyte. This is essentially the case for C₁₄EES, but not for isoC₁₈MES (see figure S2 in the Supporting Information). The origin of these differences are uncertain and are often discussed in the context of other isotherm forms, such as Van der Waals or Frumkin (44) which accommodate a strong interaction between neighbouring molecules which can be repulsive or attractive. These changes can also be associated with clustering between surface molecules to form a patchy surface at partial coverage. This has also, in part, been considered by Fainerman and Miller (45), in an evaluation of surface pressure changes due to n' mer formation at the surface. However, from the NR measurements, and it's relative insensitivity to patch size in this regime, it is difficult to confirm or exclude that possibility.

(4) SUMMARY / CONCLUSION

NR and ST have been used to study the adsorption of two ester sulfonate anionic surfactants, C₁₄EES and isoC₁₈MES, at the air-water interface, and the impact of electrolyte, monovalent and multivalent, on the adsorption. The measurements extend previous measurements on the methyl ester sulfonate surfactants (27, 36, 37, 47), and in particular further explore the effect of changing the surfactant geometry, using an branched alkyl chain, and esterification of the headgroup with an ethyl group rather than a methyl group. The nature of the adsorption isotherms and the impact of electrolyte suggests that the surfactants are only weakly anionic and are acting more like non-ionic surfactant. The effect of electrolyte on the cmc is inconsistent with that interpretation and implies a significantly different strength and degree of counterion binding between the surface and the micellar phase. Although well described by a Langmuir isotherm, below the cmc the slopes of the isotherms are different, to the other MES surfactants studied (27, 37), and implies a greater adsorption efficiency. An alternative or additional interpretation of the change in the slope is the formation of surface clusters or patches, which are different and dependent upon surfactant geometry.

Contrary to the observation for the MES and SLES surfactants (33-37, 47), only limited surface multilayer formation is observed with the addition of Al^{3+} counterions. Indeed for the isoC₁₈MES only monolayer adsorption is observed. Whereas for C₁₄EES there is only a transition from S₀ to S₁, and more extended multilayer structures observed elsewhere are not observed. The lack of extended multilayer structures is not as a result of the early onset of precipitation at relatively low Al^{3+} concentrations, as observed for some longer alkyl chain surfactants (34), and in the C₁₆-C₁₈MES eutectic mixtures (37). The results imply that the Na⁺ counterion is more strongly bound for these two surfactants, and is not so readily displaced by the Al^{3+} ions. For the isoC₁₈MES surfactant the branched alkyl chain may be an additional factor, and partially hinders the formation of surface lamellar structures.

The impact of the mixed electrolytes of AlCl_3 / CaCl_2 and AlCl_3 / MgCl_2 on the evolution of the surface structure of C₁₄EES further illustrates the importance of the relative binding strengths of the associated counterions. For the AlCl_3 / MgCl_2 mixture the transition from S₀ to S₁ occurs at higher electrolyte concentration, as observed for C₁₄MES (46). Whereas for the AlCl_3 / CaCl_2 mixture a more complex evolution (as described earlier) exists. These trends indicate that changes in the headgroup structure can have quite subtle effects on the relative binding strengths of the different counterions.

Overall the results provide an important insight into how relatively subtle changes to surfactant geometry or structure can be used to manipulate surface properties and their response to monovalent and multivalent ions.

ACKNOWLEDGEMENTS

The authors acknowledge the provision of the neutron beam time on the SURF reflectometer at ISIS, and the invaluable technical and scientific support provided. The authors also thank the China Scholarship Council (CSC) for their financial support.

SUPPORTING INFORMATION

Supporting information is provided online in the form of tables of model parameters and additional figures.

REFERENCES

- (1) J J Scheibel, The evolution of anionic surfactant technology to meet the requirements of the laundry detergent industry, *J. Surf. Deter.* 2004, 7, 319-328
- (2) Y U Yangxin, Z Jin, A E Bayley, Development of surfactants and builders in detergent formulations, *Chin. J. Chem. Eng.* 2008, 16, 517-527
- (3) J F Scamehorn in 'Phenomena in mixed surfactant systems', Ed J F Scamehorn, ACS Symp. Ser. 311, ACS, Washington DC, 1988
- (4) M Rosen in 'Phenomena in mixed surfactant systems', Ed J F Scamehorn, ACS Symp. Ser. 311, ACS, Washington DC, 1988
- (5) K L Steller, J F Scamehorn, Surfactant precipitation in aqueous solutions containing mixtures of anionic and non-ionic surfactants, *J. Am. Oil Chem. Soc.* 1986, 63, 566-574
- (6) P Paton-Morales, F I Talens-Alessen, Effect of ionic strength and competitive adsorption of Na^+ on the flocculation of lauryl sulfate micelles with Al^{3+} , *Langmuir*, 2001, 17, 6059-6064
- (7) B L Chou, J H Bae, Surfactant precipitation and redissolution in brine, *J. Coll. Int. Sci.* 1983, 96, 192-203
- (8) J F Scamehorn, S D Christian, R T Ellington, in 'Surfactant based separation processes', J F Scamehorn, J H Harwell Eds, Surfactant Science Series, Vol 33, 1989, Marcel Dekker, NY
- (9) P Somasundaran, K P Ananthapadmanbhan, M S Celik, Precipitation – redissolution phenomena in sulfonate-aluminium chloride solutions, *Langmuir*, 1988, 4, 1061-1063
- (10) A. Sein, J. B. F. N. Engberts, E. van der Linden, J. van der Pas, Lyotropic phases of dodecylbenzene sulfonates with different counterions in water, *Langmuir*, 1996, 12, 2913-2923
- (11) R G Alargova, K D Danov, P A Kralchevsky, G Broze, A Mahreteab, Growth of giant rodlike micelles of ionic surfactants in the presence of Al^{3+} counterions, *Langmuir*, 1998, 14, 4036-4049
- (12) R G Alargova, V P Ivanova, P A Kralchevsky, A Mahreteab, G Broze, Growth of rodlike micelles in anionic surfactant solutions in the presence of Ca^{2+} counterions, *Coll. Surf. A*, 1998, 142, 201-218

- (13) J H Mu, G Z Li, Rheology of viscoelastic anionic micellar solutions in the presence of multivalent counterions, *Coll. Polym. Sci.* 2001, 279, 872-875
- (14) K D Danov, R D Stanimirova, P A Kralchevsky, E S Basheva, V I Ivanova, J T Petkov, Sulfonated methyl esters of fatty acids in aqueous solution: interfacial and micellar properties, *J. Coll. Int. Sci.* 2015, 457, 307-318
- (15) Z A Maurad, R Ghazali, P Siwayanan, Z Ismail, S Ahmad, α -sulfonated methyl ester as an active ingredient in palm-based powder detergents, *J. Surf. Det.* 2006, 9, 161-167
- (16) L Cohen, F Soto, A Melgarejo, D W Roberts, Performance of Φ -sulfo fatty methyl ester sulfonate versus linear alkyl benzene sulfonate, secondary alkane sulfates, and α -sulfo fatty methyl ester sulfonate, *J. Surf. Det.* 2008, 11, 181-186
- (17) D W Roberts, Aquatic toxicity – are surfactant properties relevant, *J. Surf. Det.* 2000, 3, 309-315
- (18) R Ghazali, Z A Maurad, P Siwayanan, M Yusof, A Ahmad, Assessment of aquatic effects of palm-based α -sulfonated methyl esters (SME), *J. Oil. Palm Res.* 2006, 18, 225-230
- (19) R Ghazali, A Ahmad, Biodegradability and ecotoxicity of palm stearin based methyl ester sulfonates, *J. Oil Palm Res.* 2004, 16, 39-44
- (20) R Ghazali, The effect of disalt on the biodegradability of methyl ester sulfonates (MES), *J. Oil Palm Res.* 2002, 14, 45-50
- (21) S Ahmad, P Siwayanan, H A Murad, H A Aziz, H Seng Soi, Beyond biodiesel, methyl esters as the route for the production of surfactant feedstocks, *Inform.* 2007, 18, 216-220
- (22) L Cohen, F Trujillo, Synthesis, characterisation and surface properties of sulfonated methyl esters, *J. Surf. Det.* 1998, 1, 338-341
- (23) L Cohen, F Soto, M S Imura, Separation and extraction of Φ -methyl ester sulfonates: new features, *J. Surf. Det.* 2001, 4, 73-74
- (24) W Stein, H Haumann, α -sulfonated fatty acids and esters: manufacturing process, properties and applications, *JAOCs*, 1975, 52, 323-329
- (25) K Ohbu, M Fujiwara, Y Abu, Physicochemical properties of α -sulfonated fatty acid esters, *Prog. Coll. Polym. Sci.* 1998, 109, 85-92
- (26) S P Wong, W H Lim, S F Cheng, C H Chuah, Properties of sodium methyl ester α -sulfoalkylate / trimethyl ammonium bromide mixtures, *J. Surf. Det.* 2012, 15, 601-611

- (27) H Xu, P X Li, K Ma, R J T Welbourn, J Penfold, D W Roberts, R K Thomas, J T Petkov, Adsorption of methyl ester sulfonate at the air-water interface: can limitations in the application of the Gibbs equation be overcome by 'computer purification', *Langmuir*, 2017, 33, 9944-9953
- (28) R K Thomas, J Penfold, Multilayering of surfactant systems at the air-water dilute aqueous solution interface, *Langmuir*, 2015, 31, 7440-7456
- (29) J Penfold, R K Thomas, C C Dong, I Tucker, K Metcalfe, S Golding, I Grillo, Equilibrium surface adsorption behaviour in complex anionic / nonionic surfactant mixtures, *Langmuir*, 2007, 23, 10140-10149
- (30) I Tucker, J Penfold, R K Thomas, C C Dong, S Golding, C Gibson, I Grillo, Surface and solution properties of anionic / nonionic surfactant mixtures of alkylbenzene sulfate and triethyleneglycol decyl ether, *Langmuir*, 2010, 26, 10614-10626
- (31) I Tucker, J Penfold, R K Thomas, C C Dong, S Golding, C Gibson, I Grillo, The adsorption and self-assembly of mixtures of alkylbenzene sulfate isomers and the role of divalent electrolyte, *Langmuir*, 2011, 27, 6674-6682
- (32) J T Petkov, I M Tucker, J Penfold, R K Thomas, D N Petsev, C C Dong, S Golding, I Grillo, The impact of multivalent counterions Al^{3+} on the surface adsorption and self-assembly of the anionic surfactant alkyloxyethylene sulfate and anionic / nonionic surfactant mixtures, *Langmuir*, 2010, 26, 16699-16709
- (33) H Xu, J Penfold, R K Thomas, J T Petkov, I Tucker, J R P Webster, The formation of surface multilayers at the air-water interface from sodium polyethylene glycol monoalkyl ether sulfate / $AlCl_3$ solutions: the role of the size of the polyethylene oxide group, *Langmuir*, 2013, 29, 11656-11666
- (34) H Xu, J Penfold, R K Thomas, J T Petkov, I Tucker, J R P Webster, The formation of surface multilayers at the air-water interface from sodium polyethylene glycol monoalkyl ether sulfate / $AlCl_3$ solutions: the role of alkyl chain length, *Langmuir*, 2013, 29, 12744-12753
- (35) H Xu, J Penfold, R K Thomas, J T Petkov, I Tucker, J R P Webster, I Grillo, A Terry, Ion specific effects in trivalent counterion induced surface and solution self-assembly of the anionic surfactant sodium polyethylene glycol monododecyl ether sulfate, *Langmuir*, 2014, 30, 4694-4702
- (36) H Xu, R K Thomas, J Penfold, P X Li, K Ma, R J L Welbourn, D W Robert, J T Petkov, The impact of electrolyte on the adsorption of the anionic surfactant

- methyl ester sulfonate at the air-solution interface: surface multilayer formation, *J Coll. Int. Sci.* 2018, 512, 231-238
- (37) H Xu, P X Li, K Ma, R J L Welbourn, J Douth, J Penfold, R K Thomas, D W Robert, J T Petkov, K L Choo, S Y Khoo, Adsorption and self-assembly in methyl ester sulfonate surfactants, their eutectic mixtures and the role of electrolyte, *J. Coll. Int. Sci.* 2018, 516, 456-465
- (38) R Bradbury, J Penfold, R K Thomas, I M Tucker, J T Petkov, C Jones, Enhanced perfume delivery to interfaces using surface multilayer structures, *J. Coll. Int. Sci.* 2016, 461, 352-358
- (39) SURF reflectometer at the ISIS Facility, <https://www.isis.stfc.ac.uk/instruments/SURF>
- (40) D W Roberts, Application of octanol/water partition coefficients in surfactant science: a quantitative structure-property relationship for micellisation of anionic surfactants, *Langmuir*, 2002, 18, 345-352
- (41) J R Lu, R K Thomas, J Penfold, Surfactant layers at the air-water interface; structure and composition, *Adv. Coll. Int. Sci.* 2000, 84, 143-304
- (42) A J Prosser, E I Franses, Adsorption and surface tension of ionic surfactants at the air-water interface, review and evaluation of equilibrium models, *Coll Surf A*, 2001, 178, 1-40
- (43) I Varga, R Meszaros, J Gilanyi, Adsorption of sodium alkyl sulfate homologues at the air-solution interface, *J. Phys. Chem. B* 2007, 111, 7160-7168
- (44) S Y Lin, K McKeigue, C Maldarelli, Diffusion limited interpretation of the induction period in the relaxation of surface tension due to the adsorption of straight chain, small polar group surfactants, theory and experiment, *Langmuir*, 1991, 7, 1055-1066
- (45) H Xu, K Ma, P X Li, R K Thomas, J Penfold, J R Lu, Limitations in the application of the Gibbs equation to anionic surfactants at the air-water interface: SDS and SLES above and below the cmc, *Langmuir*, 2013, 29, 9335-9351
- (46) V B Fainerman, R Miller, Surface tension isotherms for surfactant adsorption layers including surface aggregation, *Langmuir*, 1996, 12, 6011-6014
- (47) H Xu, P Li, K Ma, R J L Welbourn, J Penfold, R K Thomas, D W Roberts, J T Petkov, The role of competitive adsorption in the electrolyte induced surface ordering in methyl ester sulfonate surfactants at the air-water interface. *J. Coll. Int. Sci.* 2019, 533, 154-160

- (48) P X Li, Z X Li, H H Shen, R K Thomas, J Penfold, J R Lu, Application of the Gibbs equation to the adsorption of non-ionic surfactants and polymers at the air-water interface: comparison of the surface excess determined directly using neutron reflectivity, *Langmuir*, 2013, 29, 9324-9334